Automated Brain Extraction and Separation in Triphenyltetrazolium Chloride-Stained Rat Images

Herng-Hua Chang
Computational Biomedical Engineering Laboratory (CBEL)
Department of Engineering Science and Ocean Engineering
National Taiwan University
Taipei, Taiwan
Email: herbertchang@ntu.edu.tw

Shin-Joe Yeh
Graduate Institute of Anatomy and Cell Biology
National Taiwan University
Department of Neurology and Stroke Center
National Taiwan University Hospital
Taipei, Taiwan
Email: shinjoeyeh@gmail.com

Ming-Chang Chiang
Department of Biomedical Engineering
National Yang-Ming University
Taipei, Taiwan
Email: mcchiang@ym.edu.tw

Sung-Tsang Hsieh
Graduate Institute of Anatomy and Cell Biology
National Taiwan University
Department of Neurology and Stroke Center
National Taiwan University Hospital
Taipei, Taiwan
Email: shsieh@ntu.edu.tw

***Abstract*—Ischemic stroke is one of the leading causes of death among aged population worldwide. To understand the mechanism and damage of cerebral ischemia, the middle cerebral artery occlusion (MCAO) model in rodents has been generally adopted. For its celerity and veracity, the 2,3,5-triphenyltetrazolium chloride (TTC) staining has been widely utilized to visualize the infarct lesion. An important precursor is to segment the brain regions and compute the midline that separates the brain for subsequent processing. This paper develops an automated brain extraction and hemisphere separation framework in TTC-stained rat images captured by a smartphone. A saliency feature detection scheme associated with superpixels is exploited to extract the brain region into individual slices from the compound image. A chain of edge detection, morphological operation, and polynomial regression methods are introduced to compute the midline. Massive experiments were conducted to quantitatively evaluate the proposed framework. Experimental results indicated that our brain extraction algorithm outperformed competitive methods and our hemisphere separation scheme provided high accuracy.**

Keywords—brain extraction, hemisphere separation, image segmentation, saliency feature, TTC

I. Introduction

Ischemic stroke is one of the leading causes of death among aged population worldwide. Cerebral ischemia can lead to many injuries including energy failure, intracellular calcium overload, and cell death, which eventually result in the loss of neurological functions and permanent disabilities [1]. To understand the mechanism of cerebral ischemia, evaluate the effect of therapeutic interventions, and study the scope of behavioral manifestations, the middle cerebral artery occlusion (MCAO) model in rodents has been widely adopted. In this model, the middle cerebral artery is occluded to cause brain tissue ischemia, which results in a massive amount of cell deaths, called the infarct. Cells in the surrounding area, which are called the ischemic penumbra, continue to die several hours or even several days after injury.

The 2,3,5-triphenyltetrazolium chloride (TTC) staining has been extensively utilized to visualize the infarct and penumbra for its celerity, veracity, and cost effectiveness [2]. The colorless TTC reacts with the mitochondrial enzyme of living cells, which results in the red compound, so that the red region reveals the healthy/normal tissue as illustrated in Fig. 1. In contrast, the whiteness in the ischemic tissue reflects the absence of living cells, which indicates the infarct region. Accordingly, TTC staining is powerful for the macroscopic differentiation between ischemic and non-ischemic tissue [3]. To analyze the TTC-stained rat brain image, the first step is to extract the brain slices from the originally captured image, which contains a scale and a label. To further process the extracted brain slice, it is required to find the midline that separates the brain into two hemispheres. The hemisphere with the infarct lesion is called the ipsilateral hemisphere, whereas the other hemisphere is called the contralateral hemisphere.

Fig. 1. Representative examples of originally captured TTC-stained rat brain images (900×1600) after stroke by a smartphone.

Although there are abundant techniques in literature for brain segmentation in medical images, a specific algorithm for TTC-stained rat brain image processing has been lacking. Manual delineation [2-4] and simple thresholding [5, 6] of the rat brain and hemisphere regions on numerous images have been traditionally adopted. While manual delineation is time consuming, the outcome by thresholding approaches is

This work was supported by the Ministry of Science and Technology of Taiwan under Grant MOST 108-2221-E-002-080-MY3.

inaccurate and case-dependent, which requires heavier human intervention to complete the task. To reduce the laborious burden and obtain a clean brain, an automated and accurate method for brain extraction and separation in TTC-stained rat brain images is an urgent need. This paper proposes a fully automated algorithm to tackle the problems of brain extraction and hemisphere separation starting from originally captured TTC-stained rat brain images as shown in Fig. 1. The proposed framework consists of two phases that correspond to the two different tasks. In the first phase of brain extraction, we propose a salient region detection algorithm to efficiently segment the eight brain slices with clean boundaries. In the second phase of hemisphere separation, the midline of the brain is obtained through edge detection and morphological operation followed by polynomial regression. The major contributions of the current work are summarized as follows:

1) An automated brain extraction and hemisphere separation framework is uniquely developed.
2) Challenges to brain segmentation and partition in TTC-stained rat images are discussed.
3) A saliency feature detection scheme associated with superpixels is proposed to extract the brain slices.
4) Influences of brain distortion on the midline computation are reduced due to the hemisphere separation framework.
5) Massive experiments in fair comparison with competitive methods are conducted to evaluate the proposed algorithm.

II. Brain Extraction

A. Challenges

Apparently, as shown in Fig. 1, extracting the brain slices from the input image is challenging due to the following observations:

1) In addition to the stained brain slices, there are a scale and a label indicating the status of the subject being captured, both of which need to be discarded.
2) The color of the brain slice ranging from white, pink, to cardinal with a nonuniform distribution.
3) The background is not simple with a varying intensity distribution and the influence of light reflection.
4) The shape of the brain is irregular with broken and unclear boundaries.

To address these challenges, we propose an efficient salient region detection algorithm as described as follows.

B. Superpixel Over-Segmentation

Two essential principles in image segmentation are: preserve relevant structures and discard irrelevant details. Our first step is to segment the TTC-stained rat image so that the segmented elements exhibit similar color characteristics with comparable dimensions and salient boundaries. To achieve this, we perform over-segmentation on the TTC-stained image to construct the set of superpixels $\boldsymbol{Z} = \{z_1, \cdots, z_K\}$, where K is the number of superpixels. Considering its high efficiency and low complexity, the simple linear iterative clustering (SLIC) method [7], which adapts k-means clustering to produce superpixels, is utilized. The number of superpixels is empirically set to $K = 65$ to facilitate the following process.

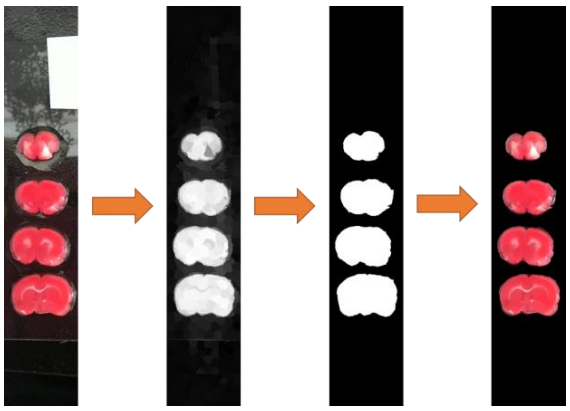

(a) (b) (c) (d)

Fig. 2. Illustration of the proposed brain extraction algorithm. (a) Input image. (b) Saliency map. (c) Binary segmentation mask. (d) Extracted brain slices. Note that the input image is a half of the originally captured TTC-stained image for better performance.

C. Saliency Feature Computation

To obtain the correct brain slices from the superpixels, we then compute a series of salient features in each superpixel z_i. Let $\boldsymbol{p}_i$ and $\boldsymbol{c}_i$ denote the position and color of the i^{th} superpixel, respectively. The color independency feature CI_i for each z_i is defined as

$$CI_i = \sum_{j=1}^{K} \|\boldsymbol{c}_i - \boldsymbol{c}_j\|^2 \alpha(\boldsymbol{p}_i, \boldsymbol{p}_j) \quad (1)$$

where $\alpha(\boldsymbol{p}_i, \boldsymbol{p}_j)$ represents the local or global proximity weight that is related to the distance between z_i and z_j. If $\alpha(\boldsymbol{p}_i, \boldsymbol{p}_j)$ is low for long distance pairs, the color independency feature is similar to the central peripheral contrast. If $\alpha(\boldsymbol{p}_i, \boldsymbol{p}_j)$ is constant, CI_i is similar to the local contrast in [8].

Generally speaking, the color of the background is more diversified whereas the foreground color is more concentrated, indicating saliency. To understand the occurrence probability of each superpixel, the spatial distribution feature SD_i in z_i is defined as

$$SD_i = \sum_{j=1}^{K} \|\boldsymbol{p}_j - \boldsymbol{\mu}_i\|^2 \beta(\boldsymbol{c}_i, \boldsymbol{c}_j) \quad (2)$$

where $\beta(\boldsymbol{c}_i, \boldsymbol{c}_j)$ represents the color affinity weight between z_i and z_j, and $\boldsymbol{\mu}_i = \sum_{j=1}^{K} \alpha(\boldsymbol{p}_i, \boldsymbol{p}_j)$ represents the weighted mean position of z_i. The closer the color and the farer the distance, the greater the SD_i value. As such, this spatial distribution feature can be used to signify the degree of the breadth of the color in z_i.

After obtaining CI_i and SD_i, the saliency feature S_i in z_i is defined using

$$S_i = CI_i \times \exp(-SD_i) \quad (3)$$

Since the range of SD_i is wider, it is incorporated into S_i with an exponential term. As the value of SD_i is higher, the spatial distribution of the color is wider, leading to a smaller saliency value. On the other hand, a greater value of CI_i corresponds to a higher degree of independency, which indicates a larger saliency value. Lastly, the final saliency feature $\tilde{S}_i$ in z_i is the weighted sum of the saliency feature using

$$\tilde{S}_i = \sum_{j=1}^{K} \omega_{ij} S_j \quad (4)$$

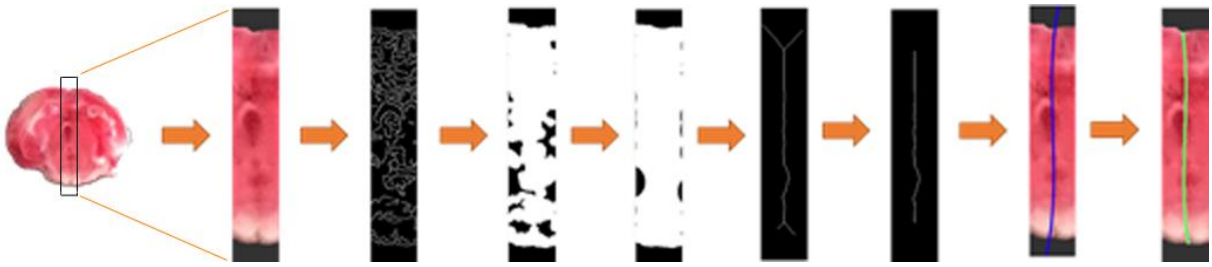

(a) (b) (c) (d) (e) (f) (g) (h) (i)

Fig. 3. Illustration of the proposed hemisphere separation algorithm. (a) Single brain image. (b) Extracted central region. (c) After Canny edge detection. (d) After morphological dilation. (e) Morphological dilation again. (f) After morphological thining. (g) After bifurcation remove. (h) After initial ploynomial regression. (i) Final midline.

where $\omega_{ij} = \frac{1}{N_i}\exp(-\frac{1}{2}(\mu\|\boldsymbol{c}_i - \boldsymbol{c}_j\|^2 + \nu\|\boldsymbol{p}_i - \boldsymbol{p}_j\|^2)$ with N_i a normalization term, μ and ν weighting factors. The above formula indicates that the final saliency feature $\tilde{S}_i$ of superpixel z_i is obtained not only by considering its own saliency property but also other superpixels being considered. Fig. 2 illustrates the entire brain extraction procedure based on the described saliency region detection methods. The obtained saliency map is further processed into a binary mask using the Otsu's method [9], where the extracted brain slices are obtained. Each individual brain slice is stored in an image with a fixed dimension after computing the vertical projection in Fig. 2 (c) for further processing.

III. Hemisphere Separation

A. Challenges

There are some challenges that need to be addressed for the hemisphere separation:

1) Due to the manual placement of the brain slice, the midline is usually not a vertical line.
2) There are few anatomically salient structures around the midline that can provide useful information for the separation.
3) The brain may be seriously distorted because of the stroke such that the midline is convoluted.

We propose the use of edge detection, morphological operation, and polynomial regression to tackle these problems.

B. Edge Detection

In each extracted rat brain image, we first compute the center of mass, based on which the central region with a width, w, is approximately obtained as illustrated in Fig. 3(a). Our assumption is that no matter how convoluted the midline is, it will always be located within this extracted region. Herein, an appropriate size is empirically determined by setting $w = 12$ pixels. As shown in Fig. 3(b), this central region is contrast-adjusted before performing edge detection. Thanks to its great efficiency, the Canny edge detection method [10] is adopted to find the edges in this region as depicted in Fig. 3(c).

C. Morphological Processing

To identify the midline, we apply a morphological dilation operation on the edge map using a disk structuring element with a radius of 3 pixels as shown in Fig. 3(d). To obtain a cleaner midline representation, the dilation operation is applied again on Fig. 3(d) followed by a hole filling operation, whose outcome is depicted in Fig. 3(e). Subsequently, the morphological thinning operation is utilized to acquire an initial estimation of the midline as illustrated in Fig. 3(f). After computing the bifurcation points, a clean curve representing the midline is extracted as shown in Fig. 3(g).

D. Polynomial Regression

Since the midline endpoints at the brain surface are irregular and case-dependent, we propose the use of polynomial regression to improve the estimation accuracy. A typical polynomial regression model can be mathematically expressed as

$$y = \beta_0 + \beta_1 x + \beta_2 x^2 + \cdots + \beta_n x^n + \varepsilon \quad (5)$$

where ε is the estimation error and β_i represents the unknown variables that need to be estimated. To estimate the parameters, the midline in Fig. 3(g) is divided into 10 segments with the order of $n = 3$ in (5). Fig. 3(h) illustrates the regressed polynomial curve, which is spanned from the top to the bottom of the central region image. After removing the extra curve, an accurate estimation of the final midline is obtained as shown in Fig. 3(i).

IV. Experimental Results

A. Image Acquisition and Evaluation Metrics

To evaluate the proposed brain extraction and hemisphere separation framework, a total of 45 rats were sacrificed for *in vitro* TTC staining. Each stained rat brain was cut into 8 slices along the coronal direction with 2 mm thick in each slice. Subsequently, as illustrated in Fig. 1, the stained slices were coded and photographed with a smartphone located at a fixed position for the experiments. To evaluate the performance of the proposed segmentation scheme, three evaluation metrics were utilized. The global similarity metric, Dice κ_D, was used to realize the segmentation efficacy using [11]

$$\kappa_D = \frac{2\theta_{TP}}{2\theta_{TP}+\theta_{FN}+\theta_{FP}} \times 100\% \quad (6)$$

where θ_{TP} means true positives, θ_{FN} means false negatives, and θ_{FP} means false positives. The gold standard of the segmentation results was provided by experts. Two local similarity metrics of sensitivity κ_{st} and sensibility κ_{sb} [12] were adopted to assess under-segmentation and over-segmentation with

$$\kappa_{st} = \frac{\theta_{TP}}{\theta_{TP}+\theta_{FN}} \times 100\% \quad (7)$$

and

$$\kappa_{sb} = 1 - \frac{\theta_{FP}}{\theta_{TP}+\theta_{FN}} \times 100\%. \quad (8)$$

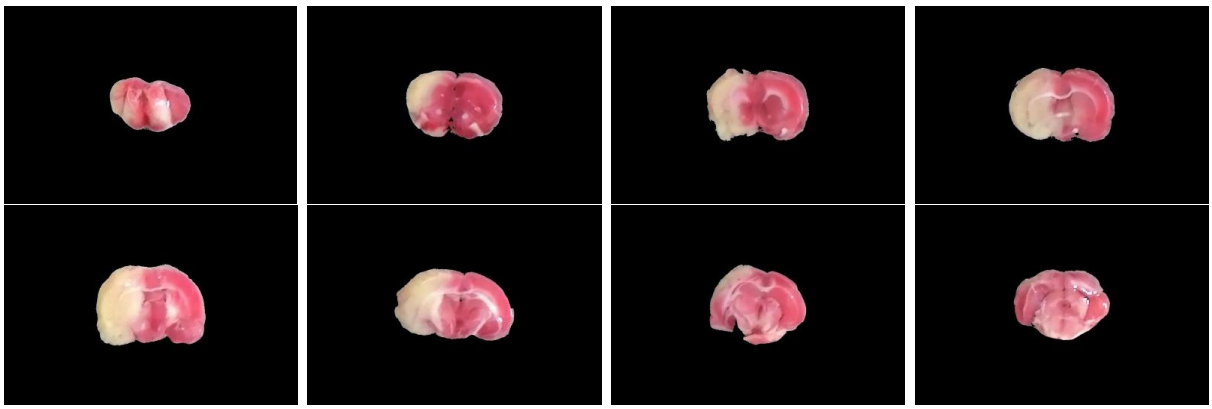

(a)

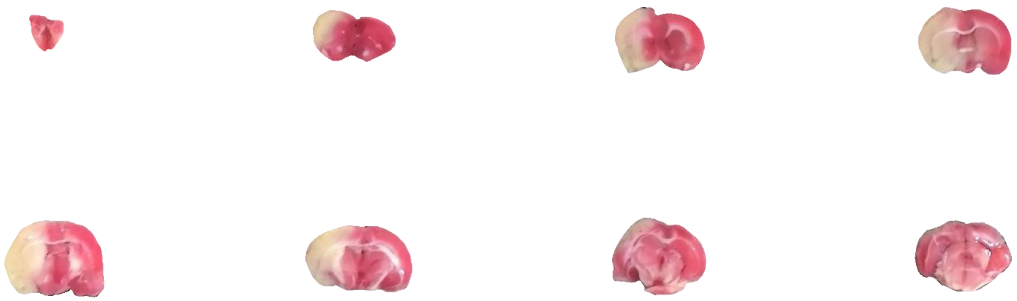

(b)

Fig. 4. Visual analyses of the brain extraction results of Subject 34. (a) The proposed algorithm. (b) The gold standard.

TABLE I. PERFORMANCE COMPARISON OF THE BRAIN EXTRACTION RESULTS.

Method	κ_D	κ_{st}	κ_{sb}
Thresholding	78.76 ± 9.14	71.32 ± 6.02	96.42 ± 2.96
Active contour	80.87 ± 6.86	73.49 ± 5.02	96.13 ± 1.94
Proposed	85.49 ± 4.36	76.78 ± 5.54	98.34 ± 0.55

TABLE II. PERFORMANCE ANALYSES OF THE BRAIN SEPARATION RESULTS.

Method	κ_D	κ_{st}	κ_{sb}
Left brain	94.99 ± 4.69	85.85 ± 4.66	98.34 ± 0.55
Right brain	93.04 ± 9.13	84.85 ± 2.86	97.24 ± 1.65
Average	94.02 ± 6.54	85.35 ± 3.65	97.79 ± 0.95

B. Brain Extraction Evaluation

We first evaluated the performance of the proposed brain extraction algorithm in the experimental image data. The input image was the originally captured TTC-stained rat brain per subject and the segmentation outcome was 8 individual brain slices. Fig. 4 visually illustrates the rat brain extraction results of a representative example in comparison with the gold standard slices. It was noted that the extracted brain slices exhibited quite clean boundaries and complete structures. The difference between the automated extraction outcome and the gold standard was larger as the brain region was getting smaller, especially for the first two slices. This was mainly due to the inevitable thickness inherited in each cut brain slice, where the upper brain region is the desired target, not the lower brain boundary. Table I presents the quantitative evaluation of the proposed algorithm along with competitive methods of the thresholding [13] and active contour [14] in massive experiments. It was obvious that our brain extraction scheme outperformed other methods with higher evaluation scores in all performance measure metrics.

C. Hemisphere Separation Evaluation

We show, in Fig. 5, the qualitative hemisphere separation results of the example in Fig. 4, where only the left brain boundaries associated with the midlines were demonstrated. The midline estimation by our algorithm was quite close to the midline delineated by experts in most brain slices. It was clear that many midlines were convoluted due to the brain distortion caused by the infarct lesion, which increased the difficulty of accurate separation. Since our hemisphere separation scheme was uniquely developed for our dataset, no available methods were able to handle the same task, leading to no comparison with other methods. Nevertheless, in Table II, we summarize the average brain separation results in our experimental image data. It was noted that the segmentation accuracy was high in both left and right brain scenarios.

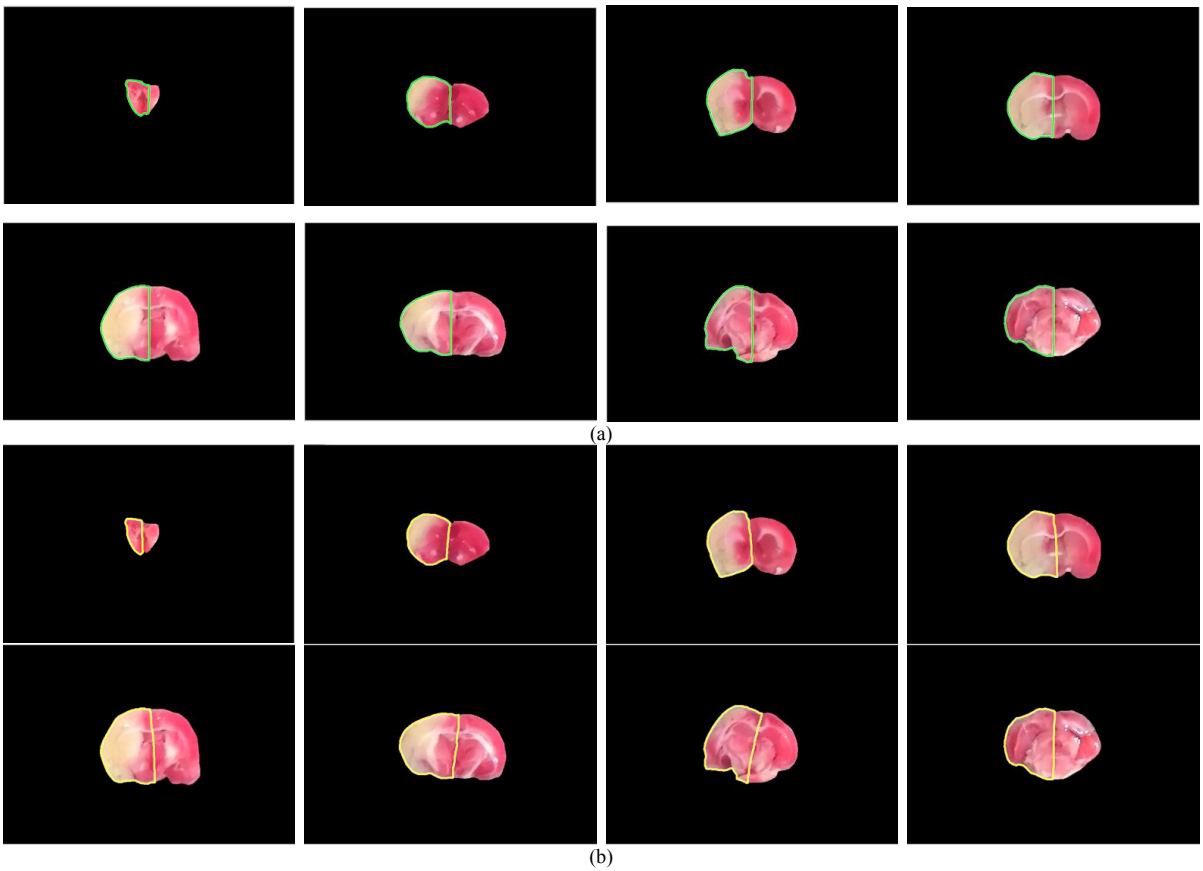

Fig. 5. Visual analyses of the hemisphere separation results of Subject 34. (a) The proposed algorithm. (b) The gold standard.

V. Conclusion

We introduced a new brain extraction and hemisphere separation algorithm in TTC-stained rat images. A saliency feature detection strategy associated with superpixels was exploited to segment the brain slices from a raw optical image captured by a smartphone. A series of edge detection, morphological processing, and polynomial regression steps were employed to compute the midline that separates the brain. The proposed algorithms were validated on massive experiments and compared with competitive methods. It was suggested that our brain extraction framework outperformed competing methods and our hemisphere separation scheme provided high segmentation accuracy. We believe that the developed methods are of potential in processing TTC-stained rat brain images captured by smartphones for further analyses.

Acknowledgment

The authors would like to thank Mr. Wei-You Lin for executing the experiments and preparing the data.

References

[1] L.-H. Zhu, Z.-P. Zhang, F.-N. Wang, Q.-H. Cheng, and G. Guo, "Diffusion kurtosis imaging of microstructural changes in brain tissue affected by acute ischemic stroke in different locations," *Neural Regeneration Research,* Research Article vol. 14, no. 2, pp. 272-279, February 1, 2019 2019.

[2] L. Li, Q. Yu, and W. Liang, "Use of 2,3,5-triphenyltetrazolium chloride-stained brain tissues for immunofluorescence analyses after focal cerebral ischemia in rats," *Pathology - Research and Practice,* vol. 214, no. 1, pp. 174-179, 2018/01/01/ 2018.

[3] A. Benedek *et al.*, "Use of TTC staining for the evaluation of tissue injury in the early phases of reperfusion after focal cerebral ischemia in rats," *Brain Research,* vol. 1116, no. 1, pp. 159-165, 2006/10/20/ 2006.

[4] Q. He *et al.*, "Total Flavonoids in Caragana (TFC) Promotes Angiogenesis and Enhances Cerebral Perfusion in a Rat Model of Ischemic Stroke," (in English), *Frontiers in Neuroscience,* Original Research vol. 12, no. 635, 2018-September-12 2018.

[5] E. J. Goldlust, R. P. Paczynski, Y. Y. He, C. Y. Hsu, and M. P. Goldberg, "Automated Measurement of Infarct Size With Scanned Images of Triphenyltetrazolium Chloride-Stained Rat Brains," *Stroke,* vol. 27, no. 9, pp. 1657-1662, 1996.

[6] E. J. Wexler, E. E. Peters, A. Gonzales, M. L. Gonzales, A. M. Slee, and J. S. Kerr, "An objective procedure for ischemic area evaluation of the stroke intraluminal thread model in the mouse and rat," *Journal of Neuroscience Methods,* vol. 113, no. 1, pp. 51-58, 2002/01/15/ 2002.

[7] R. Achanta, A. Shaji, K. Smith, A. Lucchi, P. Fua, and S. Süsstrunk, "SLIC Superpixels Compared to State-of-the-Art Superpixel Methods," *IEEE Transactions on Pattern Analysis and Machine Intelligence,* vol. 34, no. 11, pp. 2274-2282, 2012.

[8] M. Cheng, G. Zhang, N. J. Mitra, X. Huang, and S. Hu, "Global contrast based salient region detection," in *CVPR 2011*, 2011, pp. 409-416.

[9] N. Otsu, "A Threshold Selection Method from Gray-Level Histograms," *IEEE Transactions on Systems, Man, and Cybernetics,* vol. 9, no. 1, pp. 62-66, 1979.

[10] J. F. Canny, "A Computational Approach to Edge Detection," *IEEE Trans. Pattern Anal. Machine Intell.,* vol. 8, no. 6, pp. 679-698, 1986.

[11] L. R. Dice, "Measures of the amount of ecologic association between species," *Ecology,* vol. 26, no. 3, pp. 297-302, 1945.

[12] H.-H. Chang, A. H. Zhuang, D. J. Valentino, and W.-C. Chu, "Performance measure characterization for evaluating neuroimage segmentation algorithms," *Neuroimage,* vol. 47, no. 1, pp. 122-135, 2009.

[13] R. C. Gonzalez and R. E. Woods, *Digital Image Processing*, 4 ed. Pearson, 2018.

[14] T. F. Chan and L. A. Vese, "Active contours without edges," *IEEE Trans. Image Processing,* vol. 10, no. 2, pp. 266-277, 2001.